ARTICLE

AU1

Clinical evaluation of the effectiveness of asymmetric intracorneal ring with variable thickness and width for the management of keratoconus

Ricardo Cuiña Sardiña, MD, Alexandra Arango, MD, Jose F. Alfonso, MD, PhD, Juan Álvarez de Toledo, MD, PhD, David P. Piñero, PhD

Purpose: To evaluate the short-term clinical outcomes obtained with a new model of asymmetric intracorneal ring segments (ICRS) with variable thickness and base width in keratoconus.

Setting: Four Spanish ophthalmologic centers.

Design: Prospective multicenter longitudinal noncomparative clinical trial.

Methods: Thirty-one keratoconus eyes of 25 patients (age, 15 to 50 years) that underwent implantation of ICRS of variable thickness and base (AJL-pro^{+}) in 4 Spanish centers were enrolled. Visual, refractive, topographic, aberrometric, and pachymetric changes were evaluated during a 3-month follow-up. Complications were also recorded.

AU3

Results: Statistically significant changes after surgery were observed in uncorrected distance visual acuity (P = .002) and corrected distance visual acuity (CDVA) (P = .005), as well as in spherical equivalent (P = .006). At 3 months postoperatively, no loss of 2 or more lines of CDVA was observed, whereas 48.4% (15) of eyes gained ≥1 line. Statistically significant changes were observed in the steepest and mean keratometric values ($P \leq$ .047) and in the magnitude of astigmatism ($P <$ .001) of both anterior and posterior corneal surfaces. Likewise, a change to a less prolate shape of the anterior surface was found (P = .011). Primary coma was also reduced significantly at 1 month postoperatively (P = .001, mean reduction 40.1%). No serious implant-related complications occurred during the follow-up.

Conclusions: The implantation of intrastromal asymmetric ring segments of variable thickness and base width in keratoconus corneas induces a significant anterior corneal flattening, leading to refractive changes, a significant reduction of its prolate shape and irregularity, and improvement in patient's corrected distance visual acuity.

J Cataract Refract Surg 2020; ■:1–10 Copyright © 2020 Published by Wolters Kluwer on behalf of ASCRS and ESCRS

The implantation of intracorneal ring segments (ICRS) has shown to be an effective option for the visual rehabilitation of patients with keratoconus as these implants can reduce significantly corneal aberrations and irregularity.[1,2] Despite the advances in surgical and diagnostic technologies and in the nomograms of implantation, suboptimal results are still present in some cases, requiring adjustments and even the explantation of the ring segment.[3–12] More knowledge on the mechanism of action of these implants is still necessary to improve the design of the implants and their nomograms of use. Indeed, a poor correlation has been reported between the visual outcomes achieved with ICRS and tomographic measurements.[13] Some simulation models have been developed in the attempt of predicting the potential effect of ICRS, obtaining some trends that are consistent with clinical data, such as the influence of ring thickness and diameter on the level of central flattening induced and the influence of the depth of implantation.[14–16]

Currently, there are 4 main variations of intracorneal rings available internationally: ring segments with hexagonal cross-sectional profile (Intacs; Addition Technology, Inc.), ring segments with oval profile (Intacs SK; Addition Technology, Inc.), ring segments with triangular profile or variations of this profile (Ferrara rings; Ferrara Ophthalmics; Keraring; Mediphacos Ltd.), and complete rings with trapezoidal cross-sectional profile (MyoRing; Dioptex

Submitted: May 26, 2020 | Final revision submitted: October 21, 2020 | Accepted: November 7, 2020

From the Hospital Clínico San Carlos, Madrid, Spain (Cuiña Sardiña); Hospital Germans Trias i Pujol, Carretera de Canyet, Badalona, Spain (Arango); Instituto Oftalmológico Fernández-Vega, Oviedo, Spain (Alfonso); Centro de Oftalmología Barraquer, Barcelona, Spain (Álvarez de Toledo); Department of Optics, Pharmacology, and Anatomy, University of Alicante, Alicante, Spain (Piñero).

AU2

Corresponding author: David P. Piñero, PhD, Department of Optics, Pharmacology and Anatomy, University of Alicante, Crta San Vicente del Raspeig s/n 03016, San Vicente del Raspeig, Alicante, Spain. Email: david.pinyero@ua.es.

0886-3350/$ - see frontmatter
https://doi.org/10.1097/j.jcrs.0000000000000525

GmbH).[17] ICRS are available in different arc lengths, cross-sectional shapes, thickness, and diameters. With these variations, different types of keratoconus can be treated, with more limited outcomes in those eyes with more irregular corneal topographic patterns, especially in those with differences between corneal astigmatism and coma axes New models of ICRS with potentially more predictable effect in these specific cases on refractive and aberrometric outcomes have been developed and investigated.[18–24] ICRS with variable thickness and base width arise as an evolution of conventional ring segments for obtaining a more customized treatment of ectasias.[21,22] It has been suggested that ring segments with a constant thickness throughout its arc can induce an optimized astigmatic control, but not an adequate management of primary coma, which might conditionate the visual improvement achieved with them.[10] The aim of the current study was to evaluate the short-term clinical outcomes obtained with a new model of ICRS with variable thickness and base width to assess the efficacy and safety of using this type of intracorneal implant.

METHODS

Patients

This was a prospective multicenter longitudinal non-comparative clinical trial enrolling a total of 31 eyes of 25 patients with the diagnosis of keratoconus. All eyes underwent implantation of AJL-pro$^+$ asymmetric corneal ring segments of variable thickness and width (AJL Ophthalmic) in a total of 4 Spanish centers following the same protocol: Hospital Clínico San Carlos de Madrid (Madrid), Hospital Germans Trias i Pujol (Badalona), Centro de Oftalmología Barraquer (Barcelona), and Instituto Oftalmológico Fernández-Vega (Oviedo). This study was approved by the Ethics Committee of each participating institution and was performed in accordance with the ethical standards laid down in the 1964 Declaration of Helsinki. All patients provided written informed consent to be included in the study after a careful explanation of its nature, advantages, and risks.

Inclusion criteria for the study were patients aged at least 18 years, presence of keratoconus according to the standard diagnostic criteria (asymmetric topographic pattern and at least 1 of the following clinical signs on slitlamp: stromal thinning, conical protrusion of the cornea at the apex, Fleischer ring, Vogt striae, or anterior stromal scar), diagnosis of mild to moderate keratoconus according to the Amsler-Krumeich grading system (grades I to III), and inferior-superior asymmetry index of more than 1.8 diopters (D) and a discrepancy among topographic and comatic axes (between 30 and 85 degrees: irregular croissant pattern; F1 between 85 and 105 degrees: snowman pattern) (Figure 1).[25–28] Only 1 eye was included per patient, except in those cases in which a difference between right and left eyes of more than 2 grades of the Amsler-Krumeich grading system was present (significant interocular asymmetry). This was done to avoid the interference on our outcomes of the potential correlation of clinical data between fellow eyes. Exclusion criteria were severe keratoconus (grade IV, Amsler-Krumeich) previous ocular surgery, active systemic or ocular diseases, ocular media opacity, and pregnancy. No contact lens fitting was prescribed in any case during the follow-up of this study.

Examination Protocol

A complete preoperative examination was performed in all cases including anamnesis, uncorrected (UDVA) and corrected distance visual acuity (CDVA), manifest and cycloplegic refraction, slitlamp examination, tomographic analysis with the Pentacam HR system (Oculus Optikgeräte GmbH) that included evaluation of corneal topography, aberrometry, and pachymetry, infrared pupillometry, and funduscopy. Postoperatively, follow-up visits were performed the day after surgery and at 1 and 3 months after surgery. In the first postoperative day, an evaluation of UDVA and the integrity of the cornea by slitlamp was performed. The other 2 postoperative examinations included the following tests: slitlamp biomicroscopy, corneal topography and aberrometry, pachymetry, measurement of UDVA and CDVA, and manifest refraction. Total corneal aberrations considering the contribution of the combination of both anterior and posterior corneal surfaces were considered for the statistical analysis.

Ring Segments

AJL-pro$^+$ ring segments with variable thickness and width are an evolution of classical intracorneal Ferrara rings, having the same triangular cross-section (Figure 2). However, the thickness and the F2 width of the base can be modified in these new segments within a pre-defined range (Figure 2). Specifically, the ring segment models providing an optical zone of 5 mm (arc lengths of 160 and 210 degrees) present an apical length of 5.5 or 5.7 mm, a variable base width of 0.60 to 0.80 mm or 0.80 to 0.60 mm, variable thickness from 0.15 to 0.25 mm (clockwise [CW] or counterclockwise [CCW]) or from 0.15 to 0.30 mm (CW or CCW), and an orifice of 0.20 mm of diameter in each extreme of the ring. Concerning the ring segment models providing an optical zone of 6 mm, the same possibilities of variation in thickness and base width are available, but the apical length is 6.4 or 6.7 mm. The selection of the most adequate option to implant in each case was made according to the manufacturer recommendation according to its nomogram.

Surgical Technique

All surgical interventions were performed by 1 of 4 expert surgeons using topical anesthesia (2 proparacaine eyedrops, 10 minutes before surgery). Corneal incisions were placed on the steepest meridian according to the topographic map in all cases. The tunnels were created by mechanical dissection. This procedure was initiated with the creation of a mark that was used as a reference point for centration (pupil center) and a radial incision of approximately 1.8 mm in length. A calibrated diamond knife was set at approximately 80% of the thickness of the corneal area where the incision was made. From the base of such incision, pocketing hooks were used to create corneal pockets on each side of the incision, taking care to maintain a uniform depth. Afterward, a semiautomated suction ring (KV-2000 adapted for AJL Pro$^+$ rings by AJL Ophthalmic) was placed around the limbus, and 2 semicircular dissectors were placed sequentially into the lamellar pocket created to be steadily advanced by a rotational movement (CCW and CW dissectors).

Once finished the creation of the tunnels with the mechanical AU4 procedure, ring segments were inserted throughout the incision into the tunnels and centered with the help of a hook. In all patients and eyes, 31 eyes, the ring AJL Pro$^+$ was placed in the flattest meridian of the cornea (K flat). As postoperative prophylactic treatment, topical tobramycin–dexamethasone eyedrops were prescribed to be used postoperatively every 6 hours for 1 week. Likewise, a topical lubricant containing polyethylene glycol 0.4% and propylene glycol 0.3% was prescribed to be applied every 6 hours for 1 month.

The ring segments implanted in each case were selected according to the nomogram developed by Dr. Kamoun according to his own clinical experience and established by AJL as the reference nomogram for this type of segments. This nomogram is summarized in Figure 3. As shown, the diameter of the ring segment F3 was selected according to anterior corneal asphericity and the level of corneal coma. The arc length and the variation of thickness along the ring segment were selected according to the magnitude of corneal astigmatism and the discrepancy among corneal astigmatism and coma axes (Figure 3).

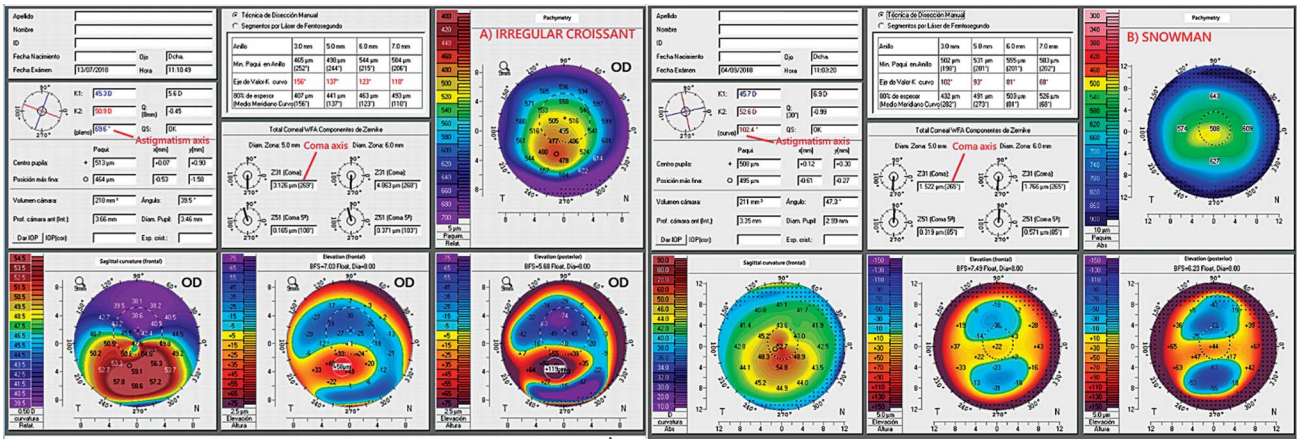

Figure 1. Corneal examination with the Pentacam system in 2 keratoconus eyes from the sample, one with an irregular croissant pattern (*A*, *left*) (discrepancy among astigmatism and comatic axes between 30 and 85 degrees) and another with a snowman pattern (*B*, *right*) (discrepancy among astigmatism and comatic axes between 85 and 105 degrees). Sagittal frontal topographic map as well as anterior and posterior elevation maps and pachymetric maps are displayed in each case. The topographic astigmatism and coma axis are remarked.

Statistical Analysis

Data analysis was performed with the commercially available software package SPSS version 22.0 (IBM Corp.). Normality of data samples was evaluated by means of the Kolmogorov-Smirnov test. For sample size estimation, the Dupont-Plummer approach was used.[29] For paired tests, a total of 30 eyes were found to be necessary to detect differences of 0.10 logarithm of the minimum angle of resolution (logMAR) in visual acuity measurements between consecutive visits, assuming a statistical power of 85% and an alpha error of 0.05.

The paired *t* test was used to assess the significance of differences between consecutive visits of normally distributed variables. The Wilcoxon test was used for non-normally distributed data instead. The Pearson or Spearman correlation coefficients were calculated for normally and non-normally distributed data, respectively, to evaluate the relationship between different clinical variables evaluated. For the analysis of refractive changes, all spherocylindrical refractions obtained were converted to vectorial notation using the power vector method described by Thibos and Horner.[30] Non parametric statistical analysis (Mann-Whitney test) was used for the comparison of the clinical outcomes obtained in eyes with irregular croissant and snowman topographic patterns. A *P* value of less than 0.05 was considered statistically significant for all statistical tests.

RESULTS

The sample included a total of 31 eyes of 25 patients (15 males and 10 females) with a mean age of 29.0 years (SD: 9.4, median: 29, range: 15 to 50 years). A total of 15 right (48.4%) and 16 left (51.6%) eyes were included, respectively. The contribution of each clinical center to the total sample was as follows: Hospital Clínico San Carlos (14 eyes, 45.2%), Hospital Germans Trias i Pujol (13 eyes, 41.9%), Instituto Oftalmológico Fernández-Vega (2 eyes, 6.5%), and Centro de Oftalmología Barraquer (1 eye, 3.2%). Mean scotopic and photopic pupil diameters in the sample evaluated were 6.1 mm (SD: 1.2; median: 6.3; range: 3.8 to 7.8 mm) and 4.1 mm (SD: 0.9; median: 4.0; range: 2.5 to 5.6 mm), respectively. Concerning the topographic pattern, a total of 26 eyes (86.7%) showed an irregular croissant pattern, whereas only 4 eyes (13.3%) showed a snowman pattern.

The most implanted segment was 150 to 250 μm CW arc 160 degrees (13 segments, 38.2%). The distribution of the rest of implants used was as follows: 150 to 300 μm CW arc 160 degrees (3 segments, 8.8%), 150 to 250 μm CCW arc 160 degrees (8 segments, 23.5%), 150 to 300 μm CCW arc 160 degrees (9 segments, 26.5%), and 150 to 300 μm CW arc 210 degrees (1 segment, 2.9%). Furthermore, in 4 eyes (12.9%), 2 segments with the same magnitude of thickness variation but opposite progression of thickness were implanted (150 to 250 μm CW-CCW arc 160 degrees in the same eye).

Visual and Refractive Changes

Table 1 summarizes the visual and refractive data obtained in the evaluated sample during the follow-up. At 1 month after surgery, there were statistically significant changes in UDVA (P = .002), spherical equivalent (P = .006), and overall blur strength (P = .001), with no additional significant changes afterward. Likewise, at 3 months postoperatively, a statistically significant change was observed in sphere (P = .007) and CDVA (P = .005). Furthermore, at 3 months after surgery, a change in the limit of statistical significance was observed for manifest cylinder (P = .054), but without significant changes associated in the power vector components of astigmatism ($P \geq .267$).

The percentage of eyes achieving a UDVA of 0.30 logMAR or better changed from 16.1% (5) preoperatively to 51.6% (16) at 3 months after surgery (Figure 1). Concerning CDVA, the percentage of eye achieving values of 0.10 logMAR or better changed from 58.1% (18) preoperatively to 74.2% (23) at 3 months after surgery (Figure 4). At 3 months postoperatively, loss of 2 or more lines of CDVA was not observed in any case (Figure 5). In contrast, 48.4% (15) of eyes gained 1 or more lines of CDVA (Figure 5). No statistically significant differences were found between eyes with irregular croissant and snowman topographic patterns in terms of the visual gain achieved at 1 (P = .50) −0.03 ± and 3 months (P = .46) postoperatively.

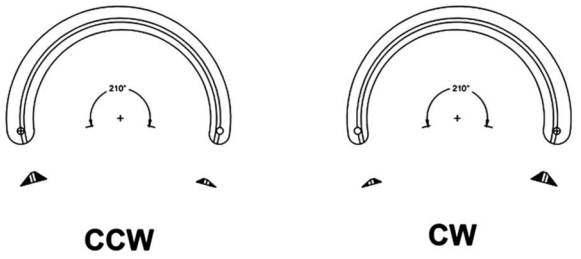

Figure 2. Frontal and cross-sectional perspective of the asymmetric intracorneal ring with variable thickness and width (AJL-pro^{+} ring segments) used in the current study. The example shows the ring segment of 210 degrees of arc length with the 2 modalities of variation of thickness, clockwise (CW) (*right*) and counterclockwise (CCW) (*left*).

Corneal Topographic Changes

T2 Table 2 summarizes the corneal topographic data obtained in the evaluated sample during the follow-up. For the anterior corneal surface, statistically significant reductions at 1 month after surgery were observed in steepest (P = .047) and mean keratometric values (P < .001) as well as in the magnitude of astigmatism (P < .001) and asphericity (P = .011), with no significant changes during the rest of follow-up ($P \geq .143$). The change in anterior flattest keratometric reading at 1 month after surgery was in the limit of statistical significance (P = .057), with no significant changes afterward (P = .146). Concerning the posterior corneal surface, similar findings were obtained, with significant changes in steepest (P < .001) and mean keratometric values (P < .001) and in the magnitude of astigmatism (P = .001) at 1 month postoperatively, and with no significant changes afterward ($P \geq .532$). No significant changes were found in posterior flattest keratometric reading and asphericity during the whole follow-up ($P \geq .150$).

Corneal Aberrometric Changes

Table 3 summarizes the corneal aberrometric data obtained T3 in the evaluated sample during the follow-up. As shown, a significant reduction in primary coma root mean square (RMS) was observed at 1 month after surgery (P = .001), with no significant reduction during the remaining follow-up (P = .915). No significant changes with surgery were detected in the rest of corneal aberrometric data evaluated ($P \geq .142$). No statistically significant differences were found in the change induced in corneal primary coma RMS at 1 (P = .11) and 3 months (P = .93) after surgery between eyes with irregular croissant and snowman topographic patterns.

Pachymetric Changes

Figure 6 shows the pachymetric changes occurring in the F6 sample evaluated. No statistically significant changes were observed in minimum and central corneal thicknesses during the follow-up ($P \geq .258$).

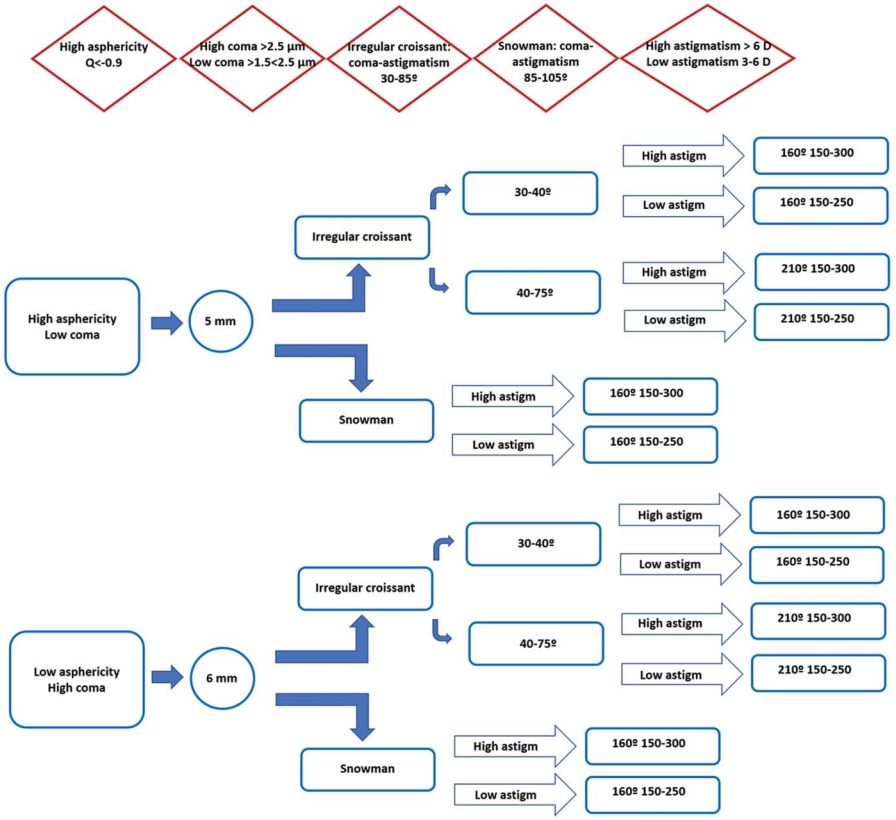

Figure 3. Nomogram used in the current study for the selection of the ring segments to implant. This nomogram was developed by Dr. Kamoun according to his own clinical experience and established by AJL as the reference nomogram for this type of segments. As shown, the diameter of the ring segment was selected according to anterior corneal asphericity and the level of corneal coma. The arc length and the variation of thickness along the ring segment were selected according to the magnitude of corneal astigmatism and the discrepancy among corneal astigmatism and coma axes.

AU6

Table 1. Visual and Refractive Changes in the Sample Evaluated.

	Preop	1 mo postop	3 mo postop	*P* value
LogMAR UDVA				Preop-1 mo .002
Mean (SD)	0.75 (0.50)	0.52 (0.41)	0.43 (0.35)	1-3 mo .13
Median (range)	0.58 (0.10, 1.70)	0.40 (0.00, 1.70)	0.34 (−0.10, 1.30)	Preop-3 mo <.001
Sphere (D)				Preop-1 mo .07
Mean (SD)	−1.56 (2.64)	−0.55 (2.32)	−0.22 (1.59)	1-3 mo .29
Median (range)	−1.63 (−9.00, 4.50)	−0.38 (−5.37, 6.00)	0.00 (−3.25, 3.00)	Preop-3 mo .007
Cylinder (D)				Preop-1 mo .10
Mean (SD)	−2.92 (2.03)	−2.16 (1.87)	−2.13 (1.79)	1-3 mo .85
Median (range)	−2.75 (−8.75, 0.00)	−1.75 (−8.00, 0.00)	−1.63 (−7.50, 0.00)	Preop-3 mo .054
Spherical equivalent (D)				Preop-1 mo .006
Mean (SD)	−3.02 (2.45)	−1.63 (2.19)	−1.28 (1.68)	1-3 mo .25
Median (range)	−3.13 (−9.00, 2.75)	−1.13 (−6.12, 3.00)	−0.81 (−5.75, 2.50)	Preop-3 mo .001
J0 (D)				Preop-1 mo .29
Mean (SD)	−0.72 (1.18)	−0.44 (0.90)	−0.49 (0.94)	1-3 mo .72
Median (range)	−0.60 (−3.54, 2.22)	−0.23 (−2.71, 1.17)	−0.12 (−2.50, 1.06)	Preop-3 mo .32
J45 (D)				Preop-1 mo .27
Mean (SD)	−0.12 (1.14)	0.12 (1.02)	0.11 (0.91)	1-3 mo .97
Median (range)	−0.14 (−2.16, 2.57)	0.03 (−3.46, 2.60)	0.06 (−3.24, 1.44)	Preop-3 mo .30
B (D)				Preop-1 mo .001
Mean (SD)	3.73 (2.06)	2.50 (1.77)	2.05 (1.47)	1-3 mo .07
Median (range)	3.68 (0.00, 9.00)	1.95 (0.00, 7.00)	1.83 (0.25, 6.86)	Preop-3 mo <.001
LogMAR CDVA				Preop-1 mo .23
Mean (SD)	0.18 (0.22)	0.15 (0.22)	0.10 (0.11)	1-3 mo .06
Median (range)	0.10 (−0.02, 1.00)	0.10 (−0.10, 1.00)	0.09 (−0.10, 0.40)	Preop-3 mo .005

B = overall blur strength; CDVA = corrected distance visual acuity; J_0 and J_{45} = power vector components of astigmatism; UDVA = uncorrected distance visual acuity

Complications

No serious complications occurred in the sample evaluated during the follow-up. Only an intraoperative complication was reported that consisted on the creation of excessively deep tunnel that generated a microperforation. In that case, ring segments were not implanted, and the patient was finally excluded from the study.

DISCUSSION

In the current multicenter study, the effect of a new modality of asymmetric ICRS has been evaluated in a sample of keratoconus eyes with irregular croissant patterns with differences between topographic and comatic axes over 20 degrees or snowman patterns, including an analysis of visual, refractive, and corneal topographic changes. In terms of visual acuity, a significant improvement in UDVA, with a significant change in spherical refraction associated, was obtained with the implantation of the ring segments evaluated. This is consistent with the findings reported with other types of asymmetric and symmetric ring segments in keratoconus cases, but without specifying the number of cases included with the corneal topographic patterns considered in the current series.[21,22,24,28,31–35] UDVA changed in our sample from a mean preoperative value of 0.75 ± 0.50 logMAR to a mean 3-month postoperative value of 0.43 ± 0.35 logMAR. Alfonso et al. reported a more

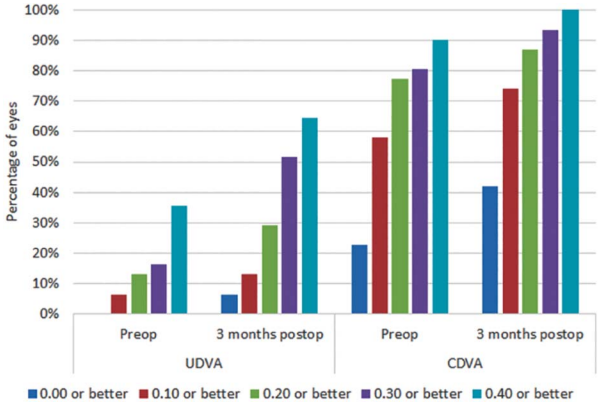

Figure 4. Distribution of preoperative and 3-month postoperative uncorrected (UDVA) and corrected distance visual acuity (CDVA).

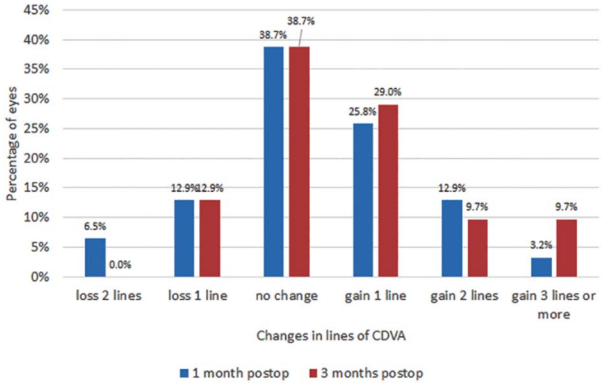

Figure 5. Distribution of changes at 1 and 3 months after surgery in corrected distance visual acuity (CDVA).

Table 2. Corneal Topographic Changes in the Sample Evaluated.

	Preop	1 mo postop	3 mo postop	*P* value
Anterior surface				
K1 (D)				Preop-1 mo .057
Mean (SD)	45.57 (2.49)	44.99 (2.58)	43.99 (3.24)	1-3 mo .15
Median (range)	45.13 (41.00, 53.60)	44.57 (41.10, 51.80)	44.00 (31.70, 50.00)	Preop-3 mo .047
K2 (D)				Preop-1 mo <.001
Mean (SD)	49.73 (3.15)	47.34 (2.51)	46.70 (2.46)	1-3 mo .19
Median (range)	49.20 (44.80, 58.00)	46.95 (43.30, 54.10)	46.60 (40.10, 53.60)	Preop-3 mo <.001
KM (D)				Preop-1 mo <.001
Mean (SD)	47.53 (2.72)	46.13 (2.41)	45.29 (2.78)	1-3 mo .15
Median (range)	47.14 (43.50, 55.70)	45.62 (43.00, 52.90)	45.37 (35.40, 51.80)	Preop-3 mo .16
Astigmatism (D)				Preop-1 mo <.001
Mean (SD)	4.15 (1.39)	2.34 (1.64)	2.72 (1.84)	1-3 mo .14
Median (range)	3.85 (1.50, 7.00)	1.78 (0.10, 5.50)	1.80 (0.50, 8.40)	Preop-3 mo <.001
Kmax (D)				Preop-1 mo .58
Mean (SD)	56.16 (4.05)	56.07 (4.29)	54.87 (4.55)	1-3 mo .031
Median (range)	56.50 (48.40, 64.50)	57.00 (46.48, 62.90)	55.70 (46.10, 64.10)	Preop-3 mo .016
Q				Preop-1 mo .011
Mean (SD)	−0.75 (0.40)	−0.46 (0.53)	−0.41 (0.65)	1-3 mo .66
Median (range)	−0.79 (−1.51, 0.54)	−0.39 (−1.70, 0.87)	−0.35 (−1.72, 1.90)	Preop-3 mo .047
Posterior surface				
K1 (D)				Preop-1 mo .80
Mean (SD)	−6.60 (0.58)	−6.59 (0.56)	−6.51 (0.50)	1-3 mo .33
Median (range)	−6.55 (−8.50, −5.80)	−6.60 (−8.10, −5.40)	−6.45 (−7.30, −5.50)	Preop-3 mo .38
K2 (D)				Preop-1 mo <.001
Mean (SD)	−7.53 (0.63)	−7.28 (0.58)	−7.25 (0.50)	1-3 mo .63
Median (range)	−7.50 (−9.20, −6.40)	−7.20 (−8.70, −6.30)	−7.20 (−8.30, −6.30)	Preop-3 mo <.001
KM (D)				Preop-1 mo .008
Mean (SD)	−7.04 (0.58)	−6.89 (0.54)	−6.86 (0.46)	1-3 mo .61
Median (range)	−7.02 (−8.80, −6.10)	−6.87 (−8.40, −5.80)	−6.80 (−7.80, −5.90)	Preop-3 mo .025
Astigmatism (D)				Preop-1 mo .001
Mean (SD)	0.93 (0.33)	0.69 (0.42)	0.74 (0.39)	1-3 mo .53
Median (range)	0.90 (0.30, 1.70)	0.60 (0.00, 1.50)	0.70 (0.20, 1.80)	Preop-3 mo .032
Q				Preop-1 mo .15
Mean (SD)	−1.01 (1.24)	−0.61 (0.58)	−0.52 (0.59)	1-3 mo .35
Median (range)	−0.72 (−6.97, 0.11)	−0.65 (−1.57, 0.72)	−0.53 (−1.76, 0.96)	Preop-3 mo .11

K1 = corneal power in the flattest meridian; K2 = corneal power in the steepest meridian; KM = mean corneal power; Kmax = maximum keratometric value; Q = asphericity

limited visual change from a mean preoperative value of 0.76 ± 0.41 logMAR to a mean postoperative value of 0.53 ± 0.46 logMAR in a sample of 41 keratoconus eyes with no coincident topographic and coma axis implanted with ICRS of constant thickness.[28] A more similar outcome compared with our series was obtained by Prisant et al. in 104 keratoconus eyes implanted with another type of ICRS of asymmetric thickness (150/250 or 200/300 μm), with a change from a mean preoperative value of 0.82 logMAR to a mean postoperative value of 0.46 logMAR.[21] In contrast, a more limited visual improvement was observed with another type of ring segment with progressive thickness, but in a sample including severe cases of keratoconus.[22] Concerning refraction, different studies have also reported significant changes in the components of manifest refraction after implantation of ICRS with different designs.[21,22,24,28,31–35] Prisant et al. reported a significant change of the spherical equivalent in keratoconus eyes implanted with another type of progressive thickness ICRS, with a change from a mean preoperative value of −3.85 D to a mean postoperative value of −1.91 D.[21] In the current study, spherical equivalent changed significantly from a mean preoperative value of −3.02 ± 2.45 D to a mean postoperative value of −1.28 ± 1.68 D.

The myopic correction induced by the asymmetric ICRS evaluated in the current study can be consistently explained by the significant reduction of the central curvature of the anterior corneal surface generated. This is consistent with the mechanism of action of this type of implants and with previous studies reporting the outcomes obtained with different modalities of ICRS.[3,14,15,21,22,24,28,31–35] Likewise, a change of higher magnitude was observed in the corneal power corresponding to the steepest meridian of the anterior corneal surface, leading to a lower difference in corneal power between flattest and steepest meridians. This may be consistent with a change in manifest astigmatism, but in some cases, there was a clear disagreement between anterior corneal and refractive astigmatism. Indeed, no

Table 3. Corneal Aberrometric Changes in the Sample Evaluated.

	Preop	1 mo postop	3 mo postop	*P* value
Higher-order RMS (μm)				Preop-1 mo .19
Mean (SD)	3.95 (2.64)	3.19 (2.45)	2.98 (2.20)	1-3 mo .73
Median (range)	3.04 (1.08, 11.29)	2.40 (0.75, 11.35)	2.46 (0.80, 13.33)	Preop-3 mo .15
Primary coma RMS (μm)				Preop-1 mo .001
Mean (SD)	3.54 (2.35)	2.06 (1.57)	2.12 (2.09)	1-3 mo .92
Median (range)	2.77 (0.89, 9.51)	1.73 (0.14, 6.83)	1.70 (0.31, 11.72)	Preop-3 mo .024
Zernike coefficient of primary spherical aberration (μm)				Preop-1 mo .14
Mean (SD)	0.04 (0.89)	0.52 (1.74)	0.41 (1.08)	1-3 mo .66
Median (range)	0.03 (−1.89, 2.44)	0.07 (−1.50, 5.72)	0.33 (−1.18, 4.06)	Preop-3 mo .13
Trefoil RMS (μm)				Preop-1 mo .88
Mean (SD)	0.94 (1.07)	0.91 (0.84)	0.90 (0.51)	1-3 mo .86
Median (range)	0.64 (0.14, 4.35)	0.72 (0.06, 4.42)	0.82 (0.20, 2.61)	Preop-3 mo .88

RMS = root mean square

significant changes with surgery were found in the power vector components of manifest astigmatism. It should be considered that the contribution of posterior corneal astigmatism to total corneal astigmatism and consequently to refractive cylinder is relevant in keratoconus eyes.[36] Furthermore, significant changes in corneal curvature and astigmatism were also detected in the posterior corneal surface with the implantation of the ring segments, as reported by previous authors with other modalities of ICRS.[37–39] These changes should be considered in future developments of the nomogram of implantation of the asymmetric thickness and base ICRS evaluated to optimize their effect on total corneal and refractive astigmatism.

Concerning asphericity, only a significant change was observed in the anterior corneal surface, with its shape changing to a less prolate profile, which was consistent with the central flattening induced. Likewise, the same trend was observed in the posterior corneal surface, but changes did not reach statistical significance. These findings are like those reported by Utine et al. in keratoconus eyes implanted with ring segments of constant thickness, concluding that ICRS implantation seemed to approximate the anterior corneal asphericity of advanced prolate shape to optimal prolate shape of a value around −0.46.[33] This change in asphericity is a crucial factor contributing to an improvement in CDVA and a reduction in some type of higher-order corneal aberrations. Indeed, in our series, a significant change in CDVA was observed at 3 months postoperatively, with 48.4% of eyes gaining 1 or more lines of CDVA. Similarly, previous investigations have also reported an improvement in CDVA after implanting different type of ring segments in keratoconus, although with some limitations in the visual gain achieved in those eyes with no coincidence between astigmatic and coma axes due mainly to a more limited control of coma aberration.[21,22,24,28,31–35] In our series, CDVA improved from a mean preoperative value of 0.18 ± 0.22 logMAR to a mean postoperative value of 0.10 ± 0.11 logMAR. Prisant et al. reported a significant change of CDVA although more limited compared with our study using another type of progressive thickness ICRS from a mean preoperative value of 0.31 logMAR to a mean postoperative value of 0.21 logMAR.[21]

The improvement in CDVA observed in the current study was associated to a significant change in corneal primary coma aberration, which is the main aberration degrading the visual quality in keratoconus eyes.[40] Esaka et al. found by means of stepwise multiple regression analysis that CDVA in keratoconus could be predicted considering the RMS of anterior corneal elevation and total coma aberration (adjusted R = 0.546).[40] In our series, primary coma RMS (6 mm diameter) changed significantly from a mean preoperative value of 3.54 ± 2.35 μm to a mean postoperative value of 2.12 ± 2.09 μm. Vega-Estrada et al. reported a lower change from 4.12 to 3.55 μm in corneal coma-like aberrations in keratoconus eyes implanted with other type of progressive thickness ICRS, concluding that further design enhancement was needed to increase the reduction of the corneal asymmetric aberrations and reduce the extrusion rate.[22] With the asymmetric ICRS evaluated in the current study, the change achieved in primary coma aberration was 40.1%, confirming the great

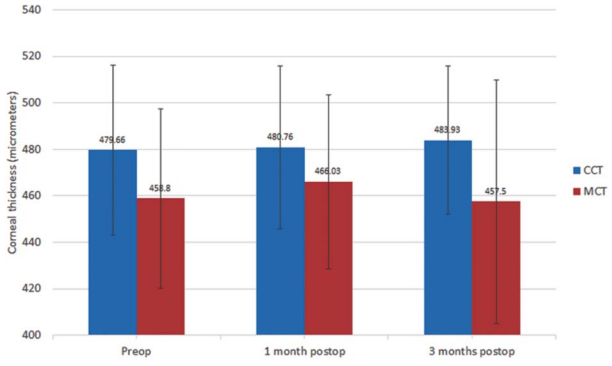

Figure 6. Pachymetric changes in the sample evaluated during the follow-up. CCT = central corneal thickness; MCT = minimum corneal thickness

efficacy of this design of ring segment to reduce this type of aberration compared with the more limited effect of symmetric ring segments in this type of aberration in eyes with large discrepancy between corneal astigmatism and coma axes.[17–20]

Finally, no severe adverse events occurred during the follow-up in the current study, confirming the safety of the implant. Only 1 complication not related specifically to the implant was reported, which was the induction in 1 case of a microperforation while creating the tunnel for the insertion of ring segments. In such case, the implantation of the ring segment was not performed, and the patient was excluded from the study. This situation has been also previously reported and normally associated with the use of a mechanical dissection for the creation of the tunnels.[41] No corneal structural alterations were detected, with no significant changes in minimum and central corneal thicknesses during the follow-up.

There are several limitations in the current study that should be acknowledged. As the femtosecond technology was not available in most of the centers involved in the study, the channels for ICRS were created by manual dissection. With this type of dissection, the intrastromal channel can run oblique in the stroma (not in an homogenous depth from the epithelial surface), with the potential of limiting or modifying the effect of the ring segments on refraction, asphericity, keratometry, and aberrations. However, it should be considered that this situation is less probable when the mechanical dissection is performed by experienced surgeons, as those involved in the current study. Monteiro et al. also found comparable visual, refractive, and aberrometric outcomes when comparing the results of Ferrara-type ring segments implanted mechanically or with femtosecond laser by an experienced surgeon.[42] In any case, future studies should be conducted using the femtosecond technology to confirm whether better or more predictable outcomes can be obtained using this technology for the creation of intrastromal channels.

As the current study was a preliminary of the effect of this new modality of ring segments, the distribution of eyes with the 2 topographic patterns (irregular croissant and snowman patterns) considered in the inclusion criteria was asymmetrical, with significantly less eyes with snowman pattern recruited. This may have been the main cause of the absence of statistical significance in the differences between eyes with snowman and irregular croissant patterns in the clinical changes observed. Future studies should be conducted to confirm this preliminary trend.

In conclusion, the implantation of AJL-pro$^+$ Ferrara rings with variable thickness and base width in keratoconus induces a significant flattening in the anterior surface, mainly in the steepest meridian, leading to a refractive change, and a significant reduction of the prolate shape and irregularity, leading to corrected distance visual improvement. Likewise, a significant change in posterior corneal curvature and astigmatism is also induced, with no structural alterations and no severe complications associated. Future studies should be conducted to evaluate the long-term outcomes of this type of implants and to optimize further the nomogram of implantation.

WHAT WAS KNOWN

- The implantation of intracorneal ring segments (ICRS) of constant thickness and base in keratoconus can reduce significantly corneal aberrations and irregularity.
- Suboptimal results are still present in some cases implanted with ICRS of constant thickness and base, requiring adjustments and even the explantation of the ring segment.
- Poor correlation has been reported between the visual outcomes achieved with ICRS and tomographic measurements, suggesting that more knowledge on the mechanism of action of these implants is still necessary.
- ICRS with variable thickness and base width are an evolution of conventional ring segments for obtaining a more customized treatment of ectasias.

WHAT THIS PAPER ADDS

- The implantation of AJL-pro$^+$ Ferrara rings with variable thickness and base width in keratoconus induces a significant flattening in the anterior surface, leading to a refractive change, and a significant reduction of its prolate shape and irregularity.
- The implantation of these asymmetric ring segments also induces significant changes in posterior corneal curvature and astigmatism.
- The implantation of these asymmetric ring segments induces a very efficient control of primary coma corneal aberration, which seems to be the main factor leading to corrected distance visual improvement.

REFERENCES

1. Benoist d'Azy C, Pereira B, Chiambaretta F, Dutheil F. Efficacy of different procedures of intra-corneal ring segment implantation in keratoconus: a systematic review and meta-analysis. Transl Vis Sci Technol 2019;8:38
2. Sakellaris D, Balidis M, Gorou O, Szentmary N, Alexoudis A, Grieshaber MC, Sagri D, Scholl H, Gatzioufas Z. Intracorneal ring segment implantation in the management of keratoconus: an evidence-based approach. Ophthalmol Ther 2019;8(suppl 1):5–14
3. Peris-Martínez C, Dualde-Beltrán C, Fernández-López E, Roig-Revert MJ, Hernández-Díaz M, Piñero DP. Effect of the variability in implantation depth of intracorneal ring segments using the femtosecond laser technology in corneal ectasia. Eur J Ophthalmol 2020;30:668–675
4. Monteiro T, Alfonso JF, Franqueira N, Faria-Correia F, Ambrósio R Jr, Madrid-Costa D. Predictability of tunnel depth for intrastromal corneal ring segments implantation between manual and femtosecond laser techniques. J Refract Surg 2018;34:188–194
5. Naftali M, Jabaly-Habib H. Depth of intrastromal corneal ring segments by OCT. Eur J Ophthalmol 2013;23:171–176
6. Pérez-Merino P, Ortiz S, Alejandre N, Jiménez-Alfaro I, Marcos S. Quantitative OCT-based longitudinal evaluation of intracorneal ring segment implantation in keratoconus. Invest Ophthalmol Vis Sci 2013;54:6040–6051
7. Lisa C, Fernández-Vega Cueto L, Poo-López A, Madrid-Costa D, Alfonso JF. Long-term follow-up of intrastromal corneal ring segments (210-degree arc length) in central keratoconus with high corneal asphericity. Cornea 2017;36:1325–1330
8. Fernández-Vega Cueto L, Lisa C, Madrid-Costa D, Merayo-Lloves J, Alfonso JF. Long-term follow-up of intrastromal corneal ring segments in paracentral keratoconus with coincident corneal keratometric, comatic, and refractive axes: stability of the procedure. J Ophthalmol 2017;2017:4058026
9. Israel M, Yousif MO, Osman NA, Nashed M, Abdelfattah NS. Keratoconus correction using a new model of intrastromal corneal ring segments. J Cataract Refract Surg 2016;42:444–454
10. Piñero DP, Alio JL, Teus MA, Barraquer RI, Uceda-Montañés A. Modeling the intracorneal ring segment effect in keratoconus using refractive,

keratometric, and corneal aberrometric data. Invest Ophthalmol Vis Sci 2010;51:5583–5591
11. Monteiro T, Mendes JF, Faria-Correia F, Franqueira N, Madrid-Costa D, Alfonso JF. Adjustment of intrastromal corneal ring segments after unsuccessful implantation in keratoconic eyes. Cornea 2018;37:182–188
12. Chan K, Hersh PS. Removal and repositioning of intracorneal ring segments: improving corneal topography and clinical outcomes in keratoconus and ectasia. Cornea 2017;36:244–248
13. Lyra JM, Lyra D, Ribeiro G, Torquetti L, Ferrara P, Machado A. Tomographic findings after implantation of Ferrara intrastromal corneal ring segments in keratoconus. J Refract Surg 2017;33:110–115
14. Flecha-Lescún J, Calvo B, Zurita J, Ariza-Gracia MÁ. Template-based methodology for the simulation of intracorneal segment ring implantation in human corneas. Biomech Model Mechanobiol 2018;17:923–938
15. Daxer A. Biomechanics of corneal ring implants. Cornea 2015;34:1493–1498
16. Lago MA, Rupérez MJ, Monserrat C, Martínez-Martínez F, Martínez-Sanchis S, Larra E, Díez-Ajenjo MA, Peris-Martínez C. Patient-specific simulation of the intrastromal ring segment implantation in corneas with keratoconus. J Mech Behav Biomed Mater 2015;51:260–268
17. Park SE, Tseng M, Lee JK. Effectiveness of intracorneal ring segments for keratoconus. Curr Opin Ophthalmol 2019;30:220–228
18. Fernández-Vega-Cueto L, Lisa C, Alfonso-Bartolozzi B, Madrid-Costa D, Alfonso JF. Intrastromal corneal ring segment implantation in paracentral keratoconus with perpendicular topographic astigmatism and comatic axis. Eur J Ophthalmol 2020 [Epub ahead of print.] doi: 10.1177/1120672120952346
19. Sedaghat MR, Momeni-Moghaddam H, Piñero DP, Akbarzadeh R, Moshirfar M, Bamdad S, Gazanchian M. Predictors of successful outcome following intrastromal corneal ring segments implantation. Curr Eye Res 2019;44:707–715
20. Peña-García P, Alió JL, Vega-Estrada A, Barraquer RI. Internal, corneal, and refractive astigmatism as prognostic factors for intrastromal corneal ring segment implantation in mild to moderate keratoconus. J Cataract Refract Surg 2014;40:1633–1644
21. Prisant O, Pottier E, Guedj T, Hoang Xuan T. Clinical outcomes of an asymmetric model of intrastromal corneal ring segments for the correction of keratoconus. Cornea 2020;39:155–160
22. Vega-Estrada A, Chorro E, Sewelam A, Alio JL. Clinical outcomes of a new asymmetric intracorneal ring segment for the treatment of keratoconus. Cornea 2019;38:1228–1232
23. Torquetti L, Cunha P, Luz A, Kwitko S, Carrion M, Rocha G, Signorelli A, Coscarelli S, Ferrara G, Bicalho F, Neves R, Ferrara P. Clinical outcomes after implantation of 320°-arc length intrastromal corneal ring segments in keratoconus. Cornea 2018;37:1299–1305
24. Al-Tuwairqi WS, Osuagwu UL, Razzouk H, AlHarbi A, Ogbuehi KC. Clinical evaluation of two types of intracorneal ring segments (ICRS) for keratoconus. Int Ophthalmol 2017;37:1185–1198
25. Piñero DP, Nieto JC, Lopez-Miguel A. Characterization of corneal structure in keratoconus. J Cataract Refract Surg 2012;38:2167–2183
26. Alió JL, Piñero DP, Alesón A, Teus MA, Barraquer RI, Murta J, Maldonado MJ, Castro de Luna G, Gutiérrez R, Villa C, Uceda-Montanes A. Keratoconus-integrated characterization considering anterior corneal aberrations, internal astigmatism, and corneal biomechanics. J Cataract Refract Surg 2011;37:552–568
27. Alfonso JF, Lisa C, Merayo-Lloves J, Fernández-Vega Cueto L, Montés-Micó R. Intrastromal corneal ring segment implantation in paracentral keratoconus with coincident topographic and coma axis. J Cataract Refract Surg 2012;38:1576–1582
28. Alfonso JF, Fernández-Vega Cueto L, Baamonde B, Merayo-Lloves J, Madrid-Costa D, Montés-Micó R. Inferior intrastromal corneal ring segments in paracentral keratoconus with no coincident topographic and coma axis. J Refract Surg 2013;29:266–272
29. Dupont WD, Plummer WD. Power and sample size calculations: a review and computer program. Control Clin Trials 1990;11:116–128
30. Thibos LN, Horner D. Power vector analysis of the optical outcomes of refractive surgery. J Cataract Refract Surg 2001;27:80–85
31. Abdellah MM, Ammar HG. Femtosecond laser implantation of a 355-degree intrastromal corneal ring segment in keratoconus: a three-year follow-up. J Ophthalmol 2019;2019:6783181
32. Kang MJ, Byun YS, Yoo YS, Whang WJ, Joo CK. Long-term outcome of intrastromal corneal ring segments in keratoconus: five-year follow-up. Sci Rep 2019;9:315
33. Utine CA, Ayhan Z, Durmaz Engin C. Effect of intracorneal ring segment implantation on corneal asphericity. Int J Ophthalmol 2018;11:1303–1307
34. Yousif MO, Said AMA. Comparative study of 3 intracorneal implant types to manage central keratoconus. J Cataract Refract Surg 2018;44:295–305
35. Sadoughi MM, Einollahi B, Veisi AR, Zare M, Sedaghat MR, Roshandel D, Einollahi N, Rezaei J. Femtosecond laser implantation of a 340-degree intrastromal corneal ring segment in keratoconus: short-term outcomes. J Cataract Refract Surg 2017;43:1251–1256
36. Montalbán R, Alio JL, Javaloy J, Piñero DP. Correlation of anterior and posterior corneal shape in keratoconus. Cornea 2013;32:916–921
37. Muftuoglu O, Aydin R, Kilic Muftuoglu I. Persistence of the cone on the posterior corneal surface affecting corneal aberration changes after intracorneal ring segment implantation in patients with keratoconus. Cornea 2018;37:347–353
38. Torquetti L, Arce C, Merayo-Lloves J, Ferrara G, Ferrara P, Signorelli B, Signorelli A. Evaluation of anterior and posterior surfaces of the cornea using a dual Scheimpflug analyzer in keratoconus patients implanted with intrastromal corneal ring segments. Int J Ophthalmol 2016;9:1283–1288
39. Söğütlü E, Piñero DP, Kubaloglu A, Alio JL, Cinar Y. Elevation changes of central posterior corneal surface after intracorneal ring segment implantation in keratoconus. Cornea 2012;31:387–395
40. Esaka Y, Kojima T, Dogru M, Hasegawa A, Tamaoki A, Uno Y, Nishida T, Nakamura T, Hara S, Ichikawa K. Prediction of best-corrected visual acuity with swept-source optical coherence tomography parameters in keratoconus. Cornea 2019;38:1154–1160
41. Piñero DP, Alio JL. Intracorneal ring segments in ectatic corneal disease: a review. Clin Exp Ophthalmol 2010;38:154–167
42. Monteiro T, Alfonso JF, Franqueira N, Faria-Correia F, Ambrósio R Jr, Madrid-Costa D. Comparison of clinical outcomes between manual and femtosecond laser techniques for intrastromal corneal ring segment implantation. Eur J Ophthalmol 2019 [Epub ahead of print.] doi: 10.1177/1120672119872367 AU5

Disclosures: *D.P. Piñero has been supported by the Ministry of Economy, Industry and Competitiveness of Spain within the program Ramón y Cajal, RYC-2016-20471. No other disclosures were reported.*